Supporting information

Adsorbate-induced structural evolution changes the mechanism of CO oxidation on a Rh/Fe_3O_4(001) model catalyst

Zdenek Jakub[1], Jan Hulva[1], Paul T. P. Ryan[2,3], David A. Duncan[2], David J. Payne[3], Roland Bliem[1], Manuel Ulreich[1], Patrick Hofegger[1], Florian Kraushofer[1], Matthias Meier[1,4], Michael Schmid[1], Ulrike Diebold[1], Gareth S. Parkinson[1]

[1] Institute of Applied Physics, TU Wien, 1040 Vienna, Austria
[2] Diamond Light Source, Harwell Science and Innovation Campus, Didcot, OX11 0DE, UK
[3] Department of Materials, Imperial College London, South Kensington, London, SW7 2AZ, UK
[4] University of Vienna, Faculty of Physics and Center for Computational Materials Science, 1090 Vienna, Austria

*corresponding author; parkinson@iap.tuwien.ac.at

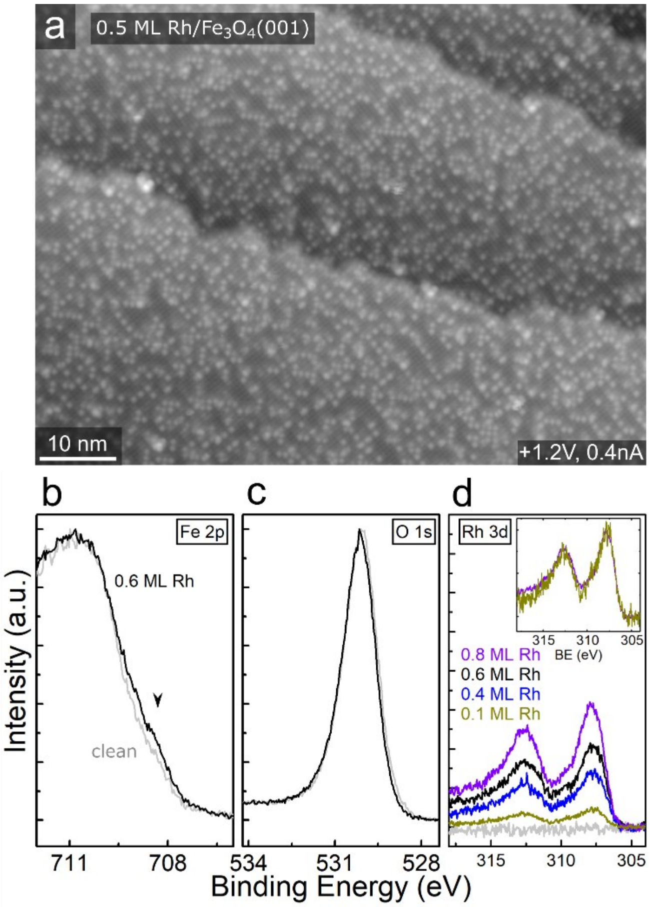

Figure S1: The Fe_3O_4(001) surface can support single Rh adatoms up to high coverages. (a) STM image of 0.5 ML Rh/Fe_3O_4(001) showing that the majority of Rh stays as single Rh_1 adatoms. (b-d) The Fe 2*p*, O 1*s* and Rh 3*d* regions of XPS spectra acquired on Rh/Fe_3O_4(001) with varying Rh coverages. Notably, the normalized spectra shown in the inset of panel (d) show that the shape and position of the Rh 3*d* peak is virtually the same for 0.1 ML and 0.8 ML coverage of Rh.

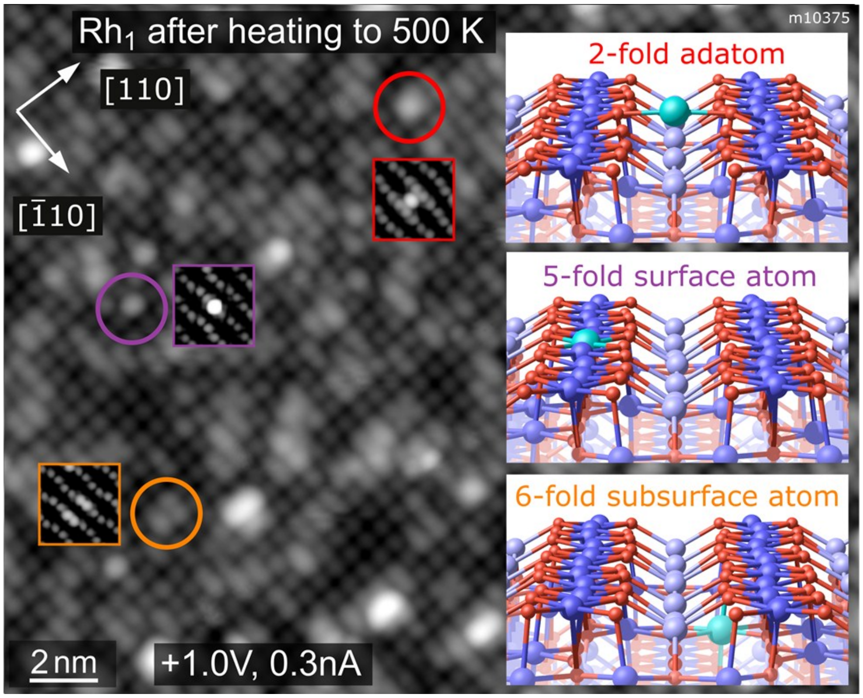

Figure S2: Comparison of species observed in STM images after heating the $Rh_1/Fe_3O_4(001)$ system to 500 K with the STM simulations previously computed for the case of $Ir_1/Fe_3O_4(001)$ which exhibits qualitatively similar behaviour. [1] The adatom incorporation was previously observed for a number of different metals on this surface, and the STM appearances look alike. [2]

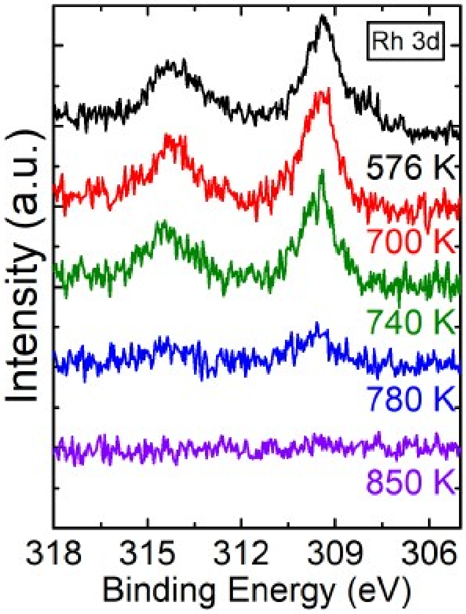

Figure S3: Annealing to elevated temperatures causes diffusion of Rh into the bulk, eventually recovering the pristine $Fe_3O_4(001)$ surface. Each of the shown spectra (Al Kα, grazing emission) was taken after annealing to the given temperature for 5–15 minutes. After the last annealing to 850 K, no Rh signal is discernible anymore.

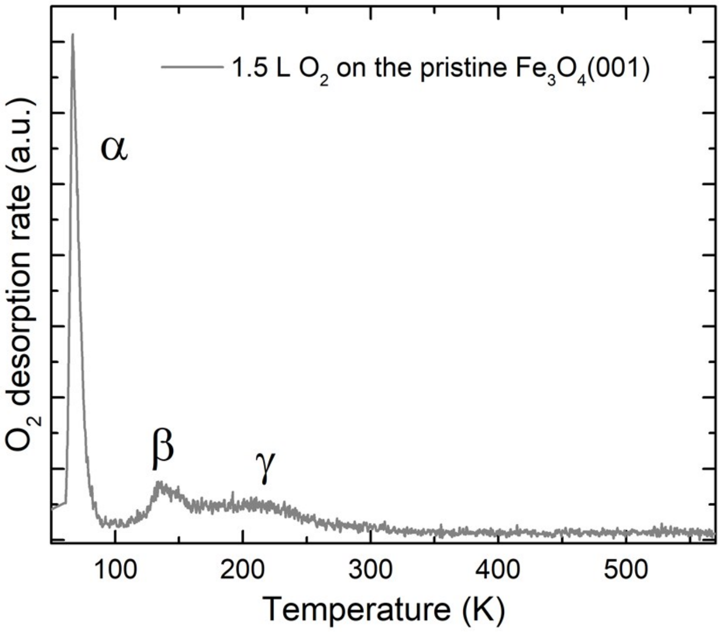

Figure S4: Oxygen TPD on the pristine $Fe_3O_4(001)$ surface exhibits a peak below 70 K corresponding to desorption of physisorbed O_2, labelled α, and two significantly smaller peaks, β and γ, presumably corresponding to O_2 adsorption on surface defects, step edges etc. In our experiments, the dosing temperature (60 K) is not low enough to fill the whole α peak and desorption already takes place before the start of the heating ramp. This leads to varying magnitude and position of the α peak due to variations in the time between dosing and start of the heating ramp.

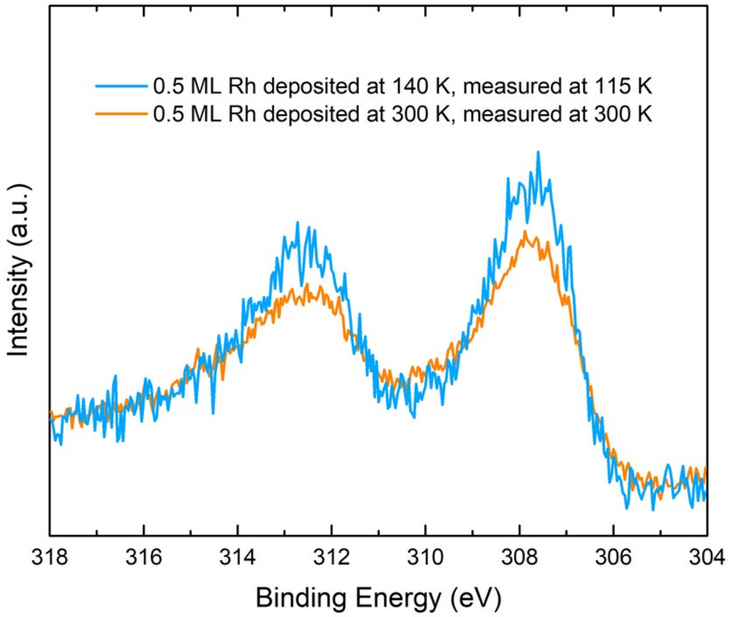

Figure S5: Deposition of Rh at lower temperature leads to the same peak positions as deposition at room temperature, but with higher signal at the peak maximum (307.7 eV) and lower signal of the shoulder located at 309.5 eV. This suggests that deposition at lower temperature yields more 2-fold coordinated Rh_1 and less incorporated Rh in comparison to room-temperature deposition.

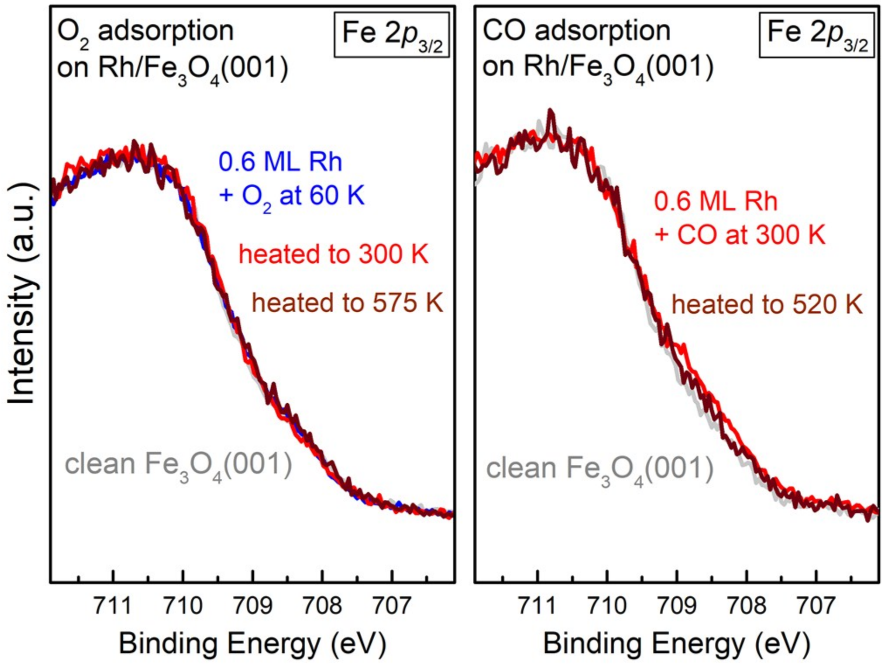

Figure S6: Details of the Fe 2$p_{3/2}$ peak corresponding to the XPS spectra shown in Figures 4 and 6 in the main text. Upon O_2 adsorption on the Rh/Fe_3O_4(001) at 60 K and heating to different temperatures, the Fe 2*p* region looks almost identical to the clean Fe_3O_4(001) surface. The temperature dependence of the Fe 2*p* peak on the Rh/Fe_3O_4(001) saturated with CO is identical to that of the Fe 2*p* peak of Rh/Fe_3O_4(001) without any CO (shown in Fig. 2c in the main text).

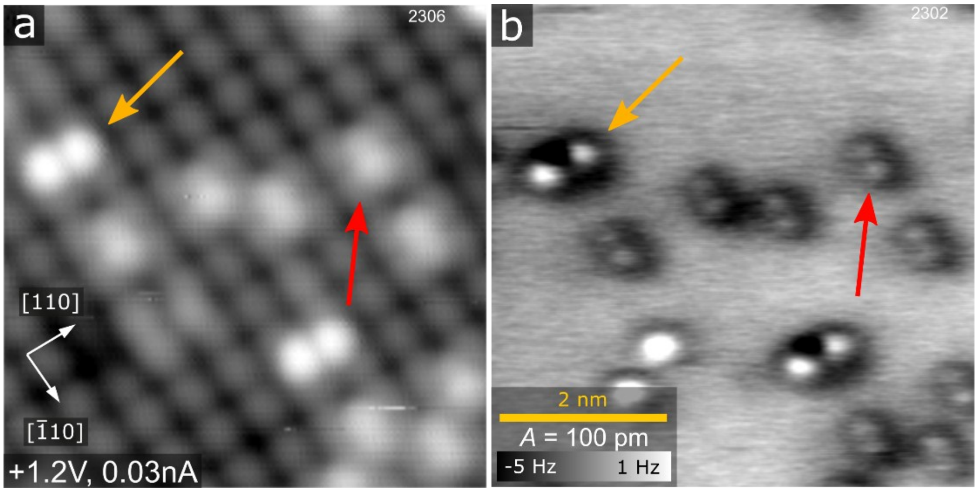

Figure S7: STM (a) and ncAFM (b) images acquired at 78 K with a CO-terminated tip on the same spot of the Rh_1/Fe_3O_4(001) surface after exposure to CO. The red arrow marks the Rh_1CO monocarbonyl species, which is resolved as a faint double protrusion in the ncAFM images. By analogy to Ir_1/Fe_3O_4(001), $^{(1)}$ this is because an additional bond to the subsurface O is formed to complete a pseudo-square-planar geometry, and the system rapidly switches between being bonded to one of the two equivalent subsurface O atoms. Yellow arrows mark the dicarbonyl $Rh_1(CO)_2$ species. These adopt the ideal square-planar geometry without formation of any additional bonds. (The rows of octrahedral Fe in the surface run in $[\bar{1}10]$ direction.)

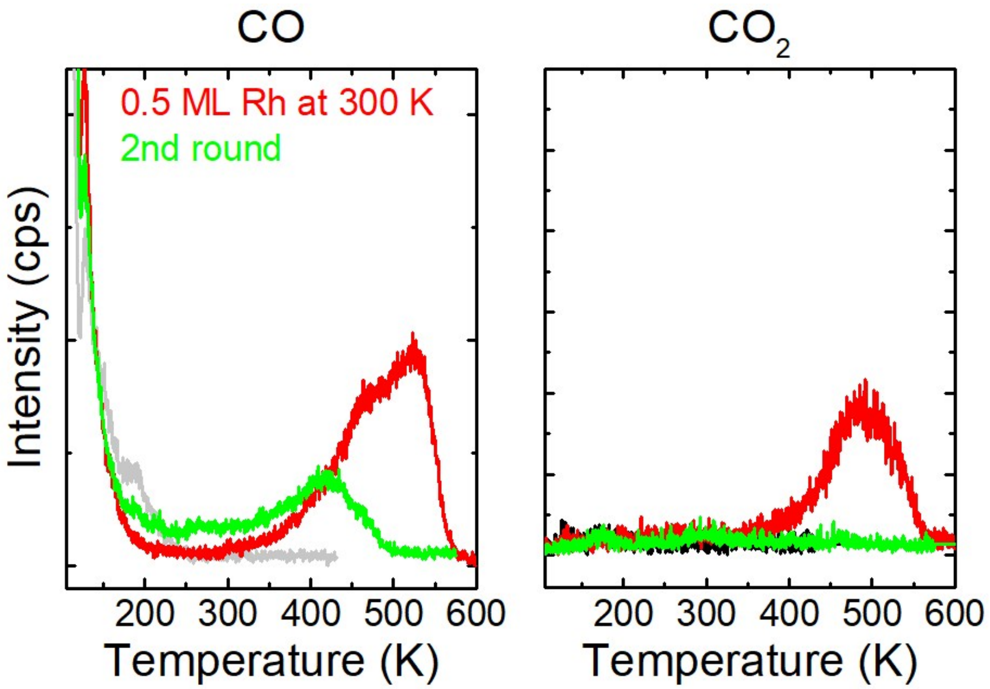

Figure S8: Comparison of the first (red) and second (green) CO TPD experiment acquired on the same 0.5 ML Rh/Fe_3O_4(001) system. In the second run (following the termination of the first TPD ramp at 600 K), the CO desorption peak is significantly smaller and has a maximum at ≈ 410 K, while no CO_2 is observed. We attribute this 410 K peak to CO desorption from Rh incorporated in the 5-fold sites in the surface. The absence of the CO peak at higher temperature and the CO_2 formation are explicable by the absence of 2-fold coordinated Rh_1 adatoms.

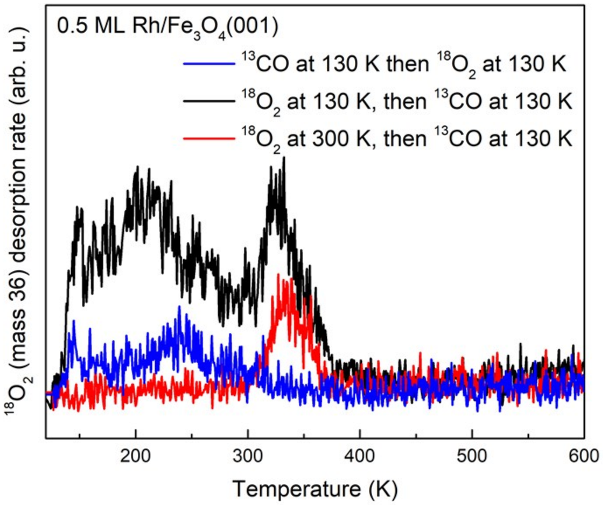

Figure S9: Desorption plots of $^{18}O_2$ (mass 36) acquired simultaneously to spectra shown in co-dosing experiments shown in Fig. 7b-d in the main text. When the surface is predosed with CO prior to the O_2 exposure, very little O_2 desorption signal is observed and the δ peak is not present. If the O_2 is dosed first at 130 K followed by CO dose at 130 K, the O_2 desorption signal resembles the TPD spectra on the pristine surface (shown in Fig. 4 in the main text). When the O_2 exposure takes place at 300 K prior to CO dose at 130 K, only the δ peak is present in the desorption spectrum, but it is significantly lower than in the previous case. This is because the dosing temperature is already in the leading edge of the desorption peak.

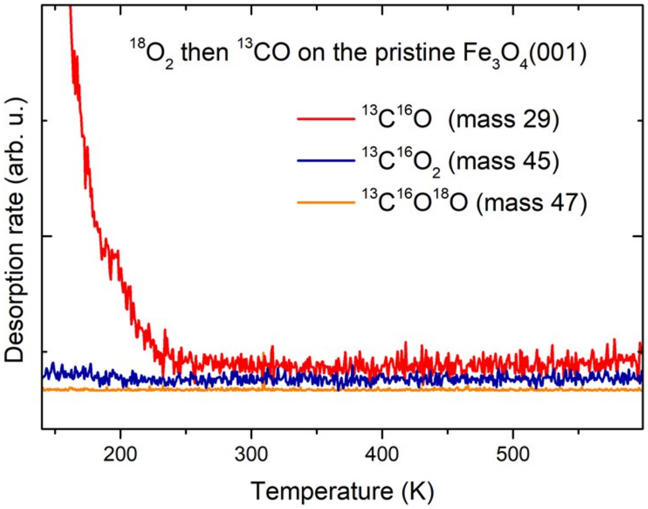

Figure S10: Sequential dosing of O_2 and CO on the pristine $Fe_3O_4(001)$ (both gases dosed at 130 K, O_2 dosed first) does not lead to production of CO_2 by any of the discussed pathways.

References

1 Jakub Z, Hulva J, Meier M, Bliem R, Kraushofer F, Setvin M, et al. Local Structure and Coordination Define Adsorption in a Model Ir_1/Fe_3O_4 Single-Atom Catalyst. Angew Chem Int Ed. 2019;58(39):13961-8.

2 Bliem R, Pavelec J, Gamba O, McDermott E, Wang ZM, Gerhold S, et al. Adsorption and incorporation of transition metals at the magnetite $Fe_3O_4(001)$ surface. Phys Rev B. 2015;92(7):075440.